Research Square

Preprints are preliminary reports that have not undergone peer review.
They should not be considered conclusive, used to inform clinical practice,
or referenced by the media as validated information.

Multi-Objective Optimization of Reservoir Rule Curves Incorporating Environmental Flow Requirements

SUKANYA J NAIR

sukanya.syamanthakam@gmail.com

IIT Palakkad: Indian Institute of Technology Palakkad https://orcid.org/0000-0002-5806-1821

Elanchezhiyan Duraisekaran

Indian Institute of Technology Madras

Sarmistha Singh

IIT Palakkad: Indian Institute of Technology Palakkad https://orcid.org/0009-0001-0048-0038

Subhasis Mitra

IIT Palakkad: Indian Institute of Technology Palakkad

Athira P

IIT Palakkad: Indian Institute of Technology Palakkad

Sudheer K P

Indian Institute of Technology Madras

Balaji Narasimhan

Indian Institute of Technology Madras

Research Article

Keywords: Optimization, Rule curve, AMALGAM, Environmental flows, Pareto-optimal

Posted Date: May 6th, 2026

DOI: https://doi.org/10.21203/rs.3.rs-9290154/v1

License: This work is licensed under a Creative Commons Attribution 4.0 International License.
Read Full License

Multi-Objective Optimization of Reservoir Rule Curves Incorporating Environmental Flow Requirements

Sukanya J Nair[1], Elanchezhiyan Duraisekaran[2], Sarmistha Singh[1,*], Subhasis Mitra[1], Athira P[1], Sudheer K P[2], Balaji Narasimhan[2]

[1] *Department of Civil Engineering, Indian Institute of Technology Palakkad, Kerala, India*
[2] *Department of Civil Engineering, Indian Institute of Technology Madras, TamilNadu, India*

*Corresponding author
Corresponding author Email: sarmistha@iitpkd.ac.in

ABSTRACT

Maintaining ecological flows in regulated rivers remains a major challenge for reservoir operations. In irrigation-dominated systems, releases from conservation reservoirs often deplete reservoir storage by the end of the irrigation season, thereby constraining the provision of environmental flows. In addition, reservoir rule curves are typically derived from historical data that do not explicitly incorporate ecological flow requirements. This study presents a multi-objective optimization framework for modifying existing reservoir rule curves to incorporate environmental flows. The rule curves of a conservation reservoir are optimized to minimize irrigation and environmental flow deficits simultaneously. The rule curve was optimized using the Multi-Algorithm Genetically Adaptive Method (AMALGAM), and the implications of selecting various trade-off solutions were discussed. The proposed approach is applied to the Malampuzha Reservoir in Kerala, India, demonstrating its potential to improve compliance with ecological flow requirements while maintaining irrigation performance. The results showed that the trade-off solution selected after the multi-objective optimization method using the Knee Point Method (KPM) and the Achievement Scalarization Function (ASF) yielded distinct optimal solutions. The reliability achieved for environmental flow was 0.90 for KPM and 0.85 for ASF, higher than the 0.5 achieved under the existing operation. In addition, the average irrigation deficit decreased from 4.97 Mm^3 to 4.72-4.75 Mm^3, and the average e-flow deficit decreased from 0.73 Mm^3 to 0.13-0.15

Mm^3.Over the 20-year simulation period, the total spill is reduced to 699.27 Mm^3 (ASF) and 721.59 Mm^3 (KPM), compared with 755.82 Mm^3 with the existing rule curves. Thus, the optimized rule curves for the conservation reservoir minimize both irrigation and the environmental flow deficits. Moreover, the reduction in spill and environmental flow deficits is achieved without compromising the irrigation releases. The developed framework can be used to update existing rule curves for conservation reservoirs that do not currently incorporate environmental flows.

Keywords: Optimization; Rule curve; AMALGAM; Environmental flows; Pareto-optimal

1. Introduction

Reservoirs are vital components of the water management system. They play a key role in redistributing available water in a timely manner, taking into account various demands. The continued demand for agriculture has reduced water availability in reservoirs, thereby limiting their ability to meet ecosystem demands (Dunn et al., 2003; Null et al., 2021). Although irrigation reservoirs can act as sources of environmental flows on an annual scale, existing reservoir operation plans do not enable them to supply the required minimum flows, especially in the dry months, without compromising the irrigation objective (Pang et al., 2018; Jo et al., 2021). Storage in the reservoir declines after irrigation supplies, leaving insufficient storage to provide ecological flows during the dry season. The construction of reservoirs has significantly reduced dry-season flows, thereby affecting the ecological balance downstream (Wineland, 2022). Maintaining minimum environmental flows in regulated rivers is a challenge that water resources planners and reservoir managers face today. Sunil et al. (2024) note that a simple modification to the release order of multipurpose reservoirs can meet minimum downstream flow requirements without significantly compromising other objectives. Hence, modifying reservoir operational rule curves

to account for environmental flow requirements is necessary to minimize adverse ecological impacts. (Wang et al., 2015). Therefore, this study focuses on incorporating environmental flows into the rule curves of conservation reservoirs using a multi-objective optimization framework.

Several researchers have studied optimal reservoir operation to allocate water for domestic supply, hydropower, flood control and ecological purposes (Dittman et al., 2009; Chen et al., 2019; Yazdian et al., 2024). Huang et al. (2016) proposed a two-stage optimization model that meets current and future economic and ecological water requirements for a water supply reservoir. Mehdipour et al. (2018) determined the optimal trade-offs between environmental flow demands and hydropower production for the Karoon 4 reservoir in Iran. Crespo et al. (2019) used a hydro-economic model to evaluate trade-offs between allocating water to economic uses and to environmental flows in a water-scarce basin. The study emphasized the need to reallocate a greater share of water for environmental purposes and to improve economic efficiency. Lu et al. (2022) studied the impact of climate change on multi-purpose reservoir operation, with emphasis on ecological water requirements. Jiang et al. (2019) developed a multi-objective storage-energy operation chart for operating multi-reservoir systems, accounting for hydropower generation, flood control, and ecological flow requirements. The minimum discharge from upstream reservoirs required to satisfy specified e-flow levels and hydropower requirements was obtained from the Pareto-optimal solutions. Qi et al. (2023) developed a multi-objective optimization model that provides an optimal trade-off between environmental flows, water supply, and power generation. They coupled only the most relevant indicators of hydrologic variability, thereby simplifying the optimization model. The environmental flows were provided at a daily time step. Wang et al. (2018) developed operation plans that combine a regular optimal operating scheme with real-time

ecological operation schemes for a multi-reservoir system. However, the studies did not analyse in detail the implications of selecting the trade-off solutions in reservoir operation.

Many studies have focused on optimizing the rule curves to incorporate ecological flow requirements, using evolutionary algorithms. Yin et al. (2010) developed a single-objective optimization model to minimize the degree of hydrologic alteration downstream of a water supply reservoir. They presented modified rule curves that incorporate inflow as a trigger, in addition to reservoir storage, for determining release rules. The model was solved using an adaptive genetic algorithm. Zhou and Gou (2013) developed optimal rule curves for a multipurpose reservoir that incorporate ecological requirements under various climate change scenarios. An adaptive genetic algorithm was used to solve the optimization problem. Taghian et al. (2014) developed a hybrid model by coupling a genetic algorithm with a reservoir simulation model to optimize the rule curves and rationing factors of a multipurpose reservoir. The conventional rule curve was coupled with a hedging rule that defined three storage zones and rationing factors to prioritize public water demand, agricultural water demand, and environmental flow requirements. They concluded that combining the hedging policy with conventional rule curves can improve reservoir performance, especially during drought periods. Ngoc et al. (2014) developed optimal rule curves for a multi-purpose reservoir to minimize the Generalised Shortage Index (GSI) using a constrained genetic algorithm. Although ecologic water allocation from hydropower and water supply reservoirs has been studied extensively, studies focusing on the trade-off between irrigation and ecologic flows are very few. Khazaipaul et al. (2019) determined the trade-off between irrigation operation benefits and environmental flow requirements for the Mahabad reservoir in Iran using a combination of a multi-objective optimization algorithm and two simulation models. The Non-Dominated Sorting Differential Evolution algorithm was used to obtain the trade-off solutions.

Jose and Srinivasan (2025a) deduced the optimal monthly E-flow targets for the Bhadra reservoir in Southern India using meta-heuristic Borg-MOEA. Jose and Srinivasan (2025b) developed a two-stage adaptive multi-objective optimization model to balance irrigation deficits and ecological demands using the Borg-MOEA. Hence, this study focuses on the trade-off between irrigation and ecological flows with a multi-objective optimization framework.

The literature review indicates that existing irrigation reservoir rule curves do not adequately account for environmental flows. Furthermore, prior studies have not explored in detail the implications of selecting trade-off solutions using various methods. Hence, this research focuses on a multi-objective optimization of the rule curves of a conservation reservoir to incorporate environmental flow requirements. Further, the study aims to explore the applicability of AMALGAM (A Multi-Algorithm Genetically Adaptive Method), an evolutionary algorithm used for the calibration of hydrologic models (Besalatpour et al., 2023) and for flood control operations in conservation reservoirs (Duraisekaran et al., 2024) in the search for optimal reservoir rule curves. Thus, the objective of the research is to modify the existing rule curves to simultaneously minimize irrigation and environmental flow deficits of a conservation reservoir. The novelty of the study lies in developing a methodology to modify existing rule curves to incorporate environmental flow requirements for a conservation reservoir, leveraging AMALGAM's search capabilities. The study also analyses the implications of selecting different trade-off solutions from the Pareto optimal set.

2. Methodology

A multi-objective optimization model is formulated to minimize the total monthly deficits in irrigation and environmental flows in a typical reservoir primarily used for irrigation. The lower and upper rule curve parameters for each month are the decision variables. The initial values of

rule curve parameters are selected such that the resulting upper and lower rule curves do not exceed and do not fall below the historic upper and lower rule curve levels. The inflows, irrigation demands, and E-flow demands for the historical period are used. A simulation model is coupled with the optimization model to determine reservoir releases for various storage levels, based on the assumed rule curves at each time step. The AMALGAM method, which has improved search efficiency and reduced computational time compared to the widely used NSGA-II (Ouyang et al., 2017), is used to determine the optimal rule curve parameters that simultaneously minimize irrigation and e-flow deficits. The number of iterations is increased until the objective function values converge. The hypervolume concept (Beume et al., 2007) is used to evaluate the spread and quality of the Pareto-optimal front. Once the Pareto-optimal front is obtained, a practically feasible solution is to be extracted. Various methods are available for selecting the optimal solution from a Pareto front. Four methods are used: the weighted-sum method, the ideal-point method, the achievement-scalarizing function method, and the knee-point method. The performance of the rule curves obtained from these methods is then compared with the existing rule curve using the indicators, reliability, resilience, and vulnerability. The long-term performance of the derived rule curves is evaluated by operating the reservoir for 100 years with synthetic inflows generated using the Thomas-Fiering model. Fig. 1 shows the overall methodology.

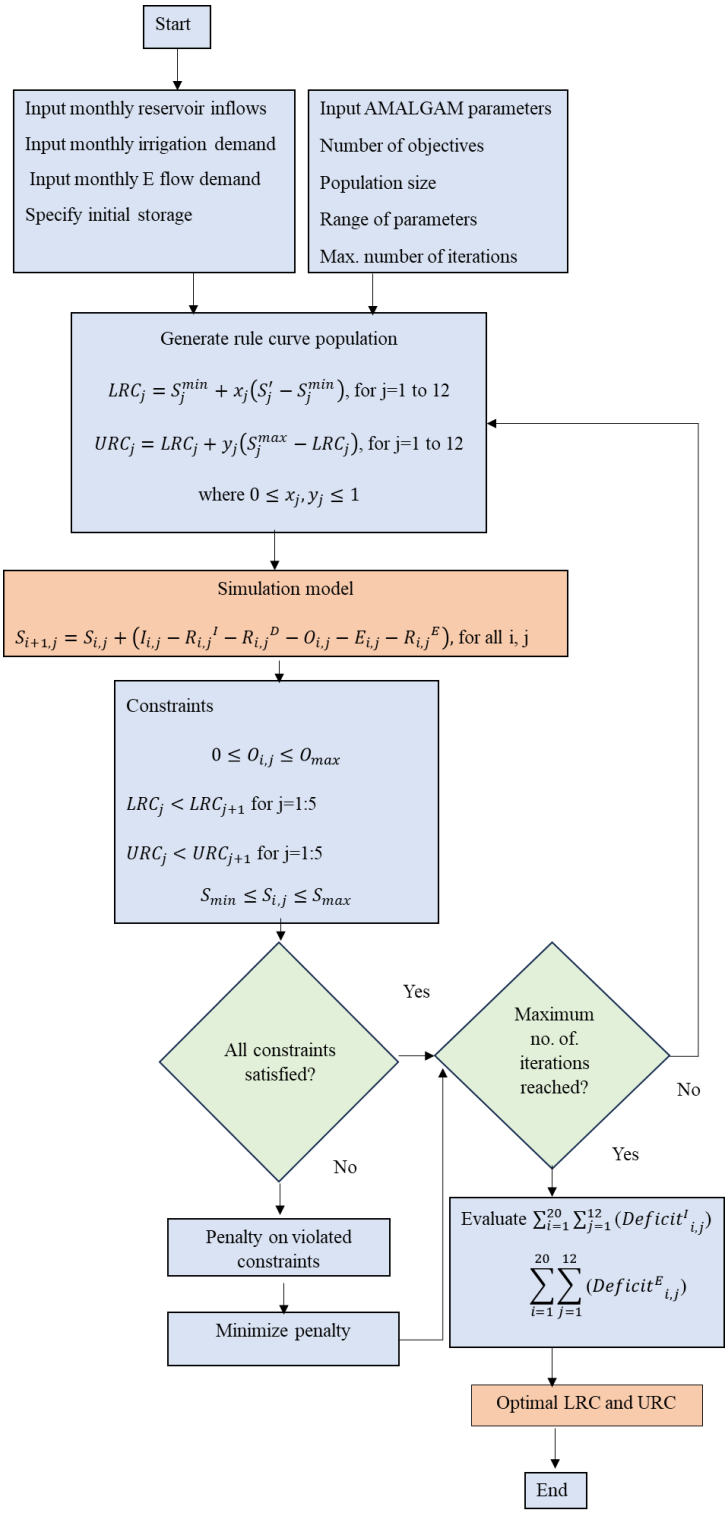


Fig. 1: Overview of the methodology adopted for the study

2.1 Optimization model

The optimization model is formulated with competing objectives: minimize the total irrigation deficit and minimize the total environmental flow deficit (hereafter referred to as the e-flow deficit).

2.1.1 Objectives

The objective functions can be defined as

$$f_1 = \text{Min} \sum_{i=1}^{20} \sum_{j=1}^{12} (Deficit^I{}_{i,j}) \quad (1)$$

$$f_2 = \text{Min} \sum_{i=1}^{20} \sum_{j=1}^{12} (Deficit^E{}_{i,j}) \quad (2)$$

where

$Deficit^I{}_{i,j}$ and $Deficit^E{}_{i,j}$ are the irrigation deficits and e-flow deficits during month j of year i.

2.1.2 Constraints

The various physical and operational constraints of the problem are:

Reservoir mass balance

$$S_{i+1,j} = S_{i,j} + \left(I_{i,j} - R_{i,j}{}^I - R_{i,j}{}^D - O_{i,j} - E_{i,j} - R_{i,j}{}^E\right), \text{ for all i, j} \quad (3)$$

where

$S_{i+1,j}$ = reservoir storage at the beginning of period i+1, j.

$S_{i,j}$ = reservoir storage at the beginning of period i, j

$I_{i,j}$ = Inflow to the reservoir during month j of year i

$O_{i,j}$ = Spill from the reservoir during month j of year i

$E_{i,j}$ = evaporation loss from reservoir during month j of year i

$R_{i,j}{}^I$ = Irrigation release from the reservoir during month j of year i

$R_{i,j}^{D}$= Release for domestic supply from the reservoir during month j of year i

$R_{i,j}^{E}$= Environmental flow release from the reservoir during month j of year limits on spillway release

The maximum release that can be made through the spillway is limited by the spillway capacity.

$$0 \leq O_{i,j} \leq O_{max} \tag{4}$$

O_{max} refers to the spillway capacity.

Limits on reservoir storage

$$S_{min} \leq S_{i,j} \leq S_{max} \tag{5}$$

The storage in the reservoir at any time, should be greater than the dead storage of the reservoir, and the storage in the reservoir shall not exceed the reservoir capacity during any stage of operation.

Limits on LRC and URC

$$LRC_j \geq S_{min} \tag{6}$$

$$URC_j \leq S_{max} \tag{7}$$

The lower bound of LRC is S_{min} , the dead storage capacity and the upper bound of URC is S_{max}, the maximum storage capacity of the reservoir.

Smoothing constraints

In order that the developed rule curves are consistent with the inflow pattern during the summer monsoon, an additional constraint is added to mimic the shape of the curves: a gradually increasing pattern from June to November, and thereafter shows a gradual decline from November to May.

For j=June to November

$$LRC_j < LRC_{j+1} \quad (8)$$

$$URC_j < URC_{j+1} \quad (9)$$

For j=December to May

$$LRC_j > LRC_{j+1} \quad (10)$$

$$URC_j > URC_{j+1} \quad (11)$$

2.2 Reservoir simulation model

The releases from the reservoir are determined by the available water, which is the sum of the initial storage in the reservoir and inflows during the period, after deducting losses. Let S_0 denote the initial storage in the reservoir, $I_{i,j}$ represent the total inflows to the reservoir during month j of year i, and losses denote the evaporation, seepage, and other losses from the reservoir. The release rules are as follows:

If $S_0 + I_{i,j} > URC_j$

$$R_{i,j}^D = D_{i,j}^D \quad (12)$$

$$R_{i,j}^I = \min\left(S_0 + I_{i,j} - R_{i,j}^D,\ D_{i,j}^I, \text{canal capacity}\right) \quad (13)$$

$$O_{i,j} = \max\left(S_0 + I_{i,j} - R_{i,j}^I - R_{i,j}^D - URC_j, 0\right) \quad (14)$$

If $LRC_j < S_0 + I_{i,j} < URC_j$

$$R_{i,j}^{D} = D_{i,j}^{D} \quad (15)$$

$$R_{i,j}^{I} = \min\left(S_0 + I_{i,j} - R_{i,j}^{D}\ ,\ D_{i,j}^{I}, \text{canal capacity}\right) \quad (16)$$

$$R_{i,j}^{E} = \min\left(S_0 + I_{i,j} - R_{i,j}^{D} - R_{i,j}^{I}\ - S_{min},\ D_{i,j}^{E}\right) \quad (17)$$

$$O_{i,j} = 0 \quad (18)$$

If $S_0 + I_{i,j}$ <LRC(i)

$$R_{i,j}^{D} = D_{i,j}^{D} \quad (19)$$

$$R_{i,j}^{E} = \min\left(S_0 + I_{i,j} - R_{i,j}^{D} - S_{min},\ D_{i,j}^{E}\right) \quad (20)$$

$$R_{i,j}^{I} = 0 \quad (21)$$

$$O_{i,j} = 0 \quad (22)$$

LRC_j and URC_j represent the storage values corresponding to the Lower Rule Curve and the Upper Rule Curve, respectively. S_{min} denotes the minimum allowable reservoir storage and $D_{i,j}^{E}$ refers to the environmental flow demand. $R_{i,j}^{D}$ and $D_{i,j}^{D}$ represent the domestic releases and domestic demands, respectively. The monthly municipal demand can be estimated based on the per capita allocation and the total population. If observed irrigation releases are available in the historical data, the monthly irrigation demand can be taken as the 75th percentile of those releases. In a similar way, the e-flow demands can be taken as the 75 th percentile value of dry month releases made during the historic period.

2.3 Optimization using AMALGAM

Generating initial rule curves is a challenging task. The initial rule curve parameters were derived from the historic reservoir operation data as follows:

$$LRC_j = S_j^{min} + x_j\left(S_j' - S_j^{min}\right), \text{ for j=1 to 12} \quad (23)$$

$$URC_j = LRC_j + y_j\left(S_j^{max} - LRC_j\right), \text{ for j=1 to 12} \quad (24)$$

$$\text{where } 0 \leq x_j, y_j \leq 1$$

LRC_j and URC_j denote the lower and upper rule curve storage for month j, respectively. S_j^{min} and S_j^{max}represent the minimum and maximum storage observed in history. S_j' is selected such that the LRC follows the existing seasonal pattern. The number of rule curve parameters (decision variables) is limited to 24, with 2 parameters x_j and y_j for each month.

AMALGAM is a multi-method search technique that combines the search capability of various algorithms. It also has the capability to create self-adaptive offspring. In this study, the various algorithms combined are Non-dominated Sorting Genetic Algorithm II (NSGA-II), Particle Swarm Optimization (PSO), Adaptive Multi-method Search (AMS), and Differential Evolution (DE). The advantage of AMALGAM is its ability to produce well-distributed Pareto-optimal solutions within a single optimization run. The method is fast, reliable, and computationally efficient (Vrugt and Robinson, 2007). The initial population is selected using Latin Hypercube Sampling, which ensures a good representation of the parameter space and increases the likelihood of convergence to a global optimal solution. The population size was set to 100, and the maximum number of function evaluations was increased progressively from 10 lakhs until the objective function values converged and a well-spread Pareto front was obtained.

2.4 Selection of a solution from the Pareto front

Solving the multi-objective optimization problem yields a Pareto-optimal front, or a set of non-inferior solutions. A Pareto-optimal solution is one in which one objective is improved at the cost of the other, or in other words, improvement in one objective can lead to a degradation in the

alternate objective considered. Finding the optimal solution on the Pareto front is subjective and depends on the decision maker's choice of which objective to prioritize. However, several methods exist to obtain an optimal solution from a Pareto front. Four different methods are discussed here. Before applying these methods, the objective function values are normalized.

In this method, each objective function value is normalized as

$$f_i = \frac{f_i - {f_{min}}^i}{{f_{max}}^i - {f_{min}}^i} \tag{25}$$

2.4.1 Weighted sum method

In the weighted sum method, multiple objectives are combined into a single objective by assigning weights to each objective based on the preference of the decision maker. If Min($f_1(x)$, $f_2(x)$, … $f_n(x)$) are the objective functions,

Weights w_i are assigned to each objective such that $w_i \geq 0$ and $\sum_{i=1}^{n} w_i = 1$.

The combined objective function is

Minimize F(x)= $\sum_{i=1}^{n} w_i f_i(x)$ (Marler and Arora, 2010)

In this study, equal weights are assigned to the objectives.

2.4.2 **Ideal point method**

The ideal point is the minimum value of each objective in a minimization problem. If $f_1(x)$, $f_2(x)$, … $f_n(x)$ are the objective function values,

Ideal point, X^*= (min $f_1(x)$, min $f_2(x)$, …, min $f_n(x)$)

The Euclidean distance of each solution to the ideal point is determined as

$$D_E = \sqrt{\sum_{i=1}^{n} (f_i(x) - X_i^*)^2} \tag{26}$$

The point closest to the ideal point is considered the optimal solution.

2.4.3 Achievement Scalarizing Function (ASF) method

In the ASF method, the deviation from the ideal point (X*) is multiplied by a weight for each solution, and the maximum of these factors is determined as the ASF for that solution. The solution corresponding to the minimum value among all ASFs is the optimal solution. A lower ASF value means that the solution is close to ideal. (Lopez et al., 2009)

ASF for a solution x is calculated as:

$$ASF(x) = max_i \left\{ \frac{f_i(x) - X^*}{w_i} \right\} \tag{27}$$

2.4.4 Knee point method

The knee point represents a solution in which a small improvement in one objective largely degrades the others. In other words, it is the point of maximum trade-off. The Pareto front is normalized, and the two extreme solutions (i.e., the best solution for each objective) are joined by a straight line. The perpendicular distance of each Pareto solution to this line is determined. The point at maximum distance is the knee point (Zhang et al., 2014).

2.5 Computing performance metrics

The performance of the reservoir with optimized rule curves and existing rule curves in the historic period was compared using the indicators- reliability, resilience and vulnerability. This is denoted by scenario H1. In order to evaluate the long-term performance, reservoir operation is carried out with the optimized and existing rule curves for synthetically generated 100-year long inflow sequence, represented as scenario S1. The 100-year inflow series was generated using the Thomas-Fiering model (Thomas and Fiering, 1962).

2.5.1 Reliability

Reliability is defined as the probability that the system is in a satisfactory state. Satisfactory state here means that there are no irrigation deficits or E-flow deficits. If we denote the reservoir state at any time, t, by the random variable X_t, then X_t belongs to either S, the set of all satisfactory states (no deficit states/successful states), or F, the set of all unsatisfactory states (deficit states/failure states). Time-based reliability,α is defined by

$$\alpha = Prob(X_t \in S) \tag{28}$$

Reliability is defined separately for irrigation and environmental flows as,

$$\alpha^I = \frac{\text{Number of months without irrigation deficit}}{\text{Total number of months of operation}} \tag{29}$$

$$\alpha^E = \frac{\text{Number of months without E-flow deficit}}{\text{Total number of months of operation}} \quad (30)$$

where α^I and α^E denote the irrigation reliability and E-flow reliability, respectively. Volume-based reliability is also used to assess the performance of reservoir operation. Volume-based reliability, β is defined as

$$\beta = \frac{R_t}{D_t} \quad (31)$$

where R_t is the volume of water released or supplied and D_t is the volume of water demand. The irrigation and E-flow reliability, represented by β^I and β^E are defined as

$$\beta^I = \frac{{R_t}^I}{{D_t}^I} \quad (32)$$

$$\beta^E = \frac{{R_t}^E}{{D_t}^E} \quad (33)$$

where ${R_t}^I$, ${R_t}^E$, ${D_t}^I$, ${D_t}^E$ are the releases and demands for irrigation and E-flow requirements respectively.

2.5.2 Resilience

Resilience describes how quickly a system is likely to recover from failure once it occurs. If γ represents resilience, it is defined by

$$\gamma = \frac{Prob(X_t \in F \; and \; X_{t+1} \in S)}{Prob(X_t \in F)} \tag{34}$$

Resilience is defined separately for irrigation and e-flow.

(35)

$$\gamma^I = \frac{\dfrac{\text{Number of transitions from F to S}}{\text{Total number of transitions}}}{\dfrac{\text{Number of failures}}{\text{Total number of months of operation}}}$$

where γ^I refers to the resilience for irrigation operation, and F refers to the state when irrigation deficits occur.

$$\gamma^E = \frac{\dfrac{\text{Number of transitions from F to S}}{\text{Total number of transitions}}}{\dfrac{\text{Number of failures}}{\text{Total number of months of operation}}} \tag{36}$$

where γ^E refers to the resilience for environmental flow operation, and F refers to the state when E-flow deficits occur.

2.5.3 Vulnerability

Vulnerability measures the severity of a failure when it occurs. Two definitions of vulnerability are commonly in existence (Jain and Bhunya, 2008). The mean value (Kjeldsen and Rosberg, 2004) and maximum value (Kundzewicz and Kindler, 1995) of the deficit event. The maximum value is adopted here. This is represented in volumetric units. If N is the total number of failure events and d_j is the duration of jth failure event, then the deficit volume is given by:

$$v_j = \sum_{t=1}^{d_j} (D_t - R_t) \tag{37}$$

Vulnerability, which is taken as either the mean value or the maximum value of the deficit event is given by,

$$V_{mean}=\frac{1}{N}\sum_{j=1}^{N} v_j \tag{38}$$

$$V_{max} = max\{v_j\} \tag{39}$$

$$V_{max}{}^{I} = D_t{}^{I} - R_t{}^{I} \tag{40}$$

$$V_{max}{}^{E} = D_t{}^{E} - R_t{}^{E} \tag{41}$$

$V_{max}{}^{I}$ and $V_{max}{}^{E}$ denote vulnerability for irrigation and environmental flow purposes respectively. In this study, V_{mean} is taken as the measure of vulnerability.

2.6 Study Area and Data Collection

For testing the optimization framework, the Malampuzha project, a major irrigation project commissioned in 1955 to irrigate 21,245 hectares in the Palakkad district of Kerala, India, was selected. It is a multi-purpose project, providing irrigation, drinking water, tourism (gardens/boating), and minor hydropower production. The water from the reservoir is heavily used for agriculture, specifically the rice paddies of Palakkad, which is considered the "granary of Kerala". Irrigation water is supplied through two main canals, the Left Bank Canal (LBC) and Right Bank Canal (RBC), which have a maximum carrying capacity of 21.24 cumecs and 4.05 cumecs, respectively.

Irrigation water requirements are limited to November through February. Occasionally, water is released for the cultivation of the first crop during the months of June, July, August, and September, when the monsoon is delayed. The domestic water supply is maintained year-round at a rate of 0.0833 Mm^3/day. Fig. 2 shows the location of the study area. The reservoir also serves to regulate floodwater during periods of excess flow. The Malampuzha reservoir has a storage capacity of 226 Mm^3 at FRL of 115.06 m. There are four gated Ogee spillways to release the floodwater.

While there is a need to balance ecological requirements with human needs, the dam is managed primarily for irrigation (supporting 21,245 ha of land) and drinking water, with environmental flows not prioritized in its operational mandate. The dam significantly restricts the flow of the Malampuzha River, a tributary of the Bharathapuzha. Observations over the past decades indicate that during the monsoon, downstream water levels have dropped significantly compared to pre-dam conditions, with some reports noting the river often does not reach the levels needed to sustain its original aquatic ecology. At present, there are no appropriate release rules for sustaining minimum environmental flows in the river. Water is released into the river during the dry period (March, April, and May) to maintain a minimum flow at the downstream ends. This supply for environmental flow regulation is provided only if sufficient storage remains after water is released for irrigation. The project struggles to balance the needs of agriculture and water supply, particularly during drought, often resulting in reduced or absent dedicated releases for the river's ecosystem. Reduced flows have contributed to reduced biodiversity and degraded aquatic habitats, affecting the river's health.

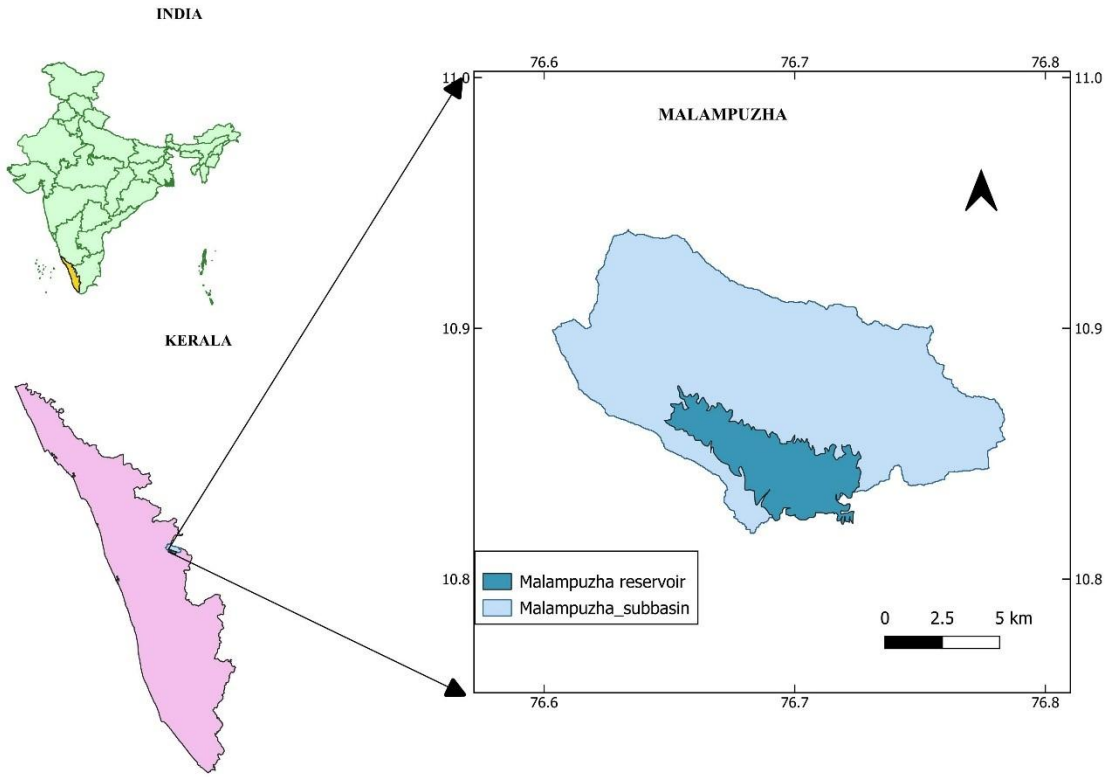


Fig. 2 Study area map

Daily reservoir operation data for the period 2000-2020 were collected from the Irrigation Department, Government of Kerala. These include daily reservoir storage and water levels, data on domestic water, canals, spillway, and environmental flow releases. The Elevation-Area-Capacity table, the monthly evaporation-loss table, and details of the reservoir's salient features were also collected. The annual variation of reservoir storage and canal release pattern is shown in Fig. 3.

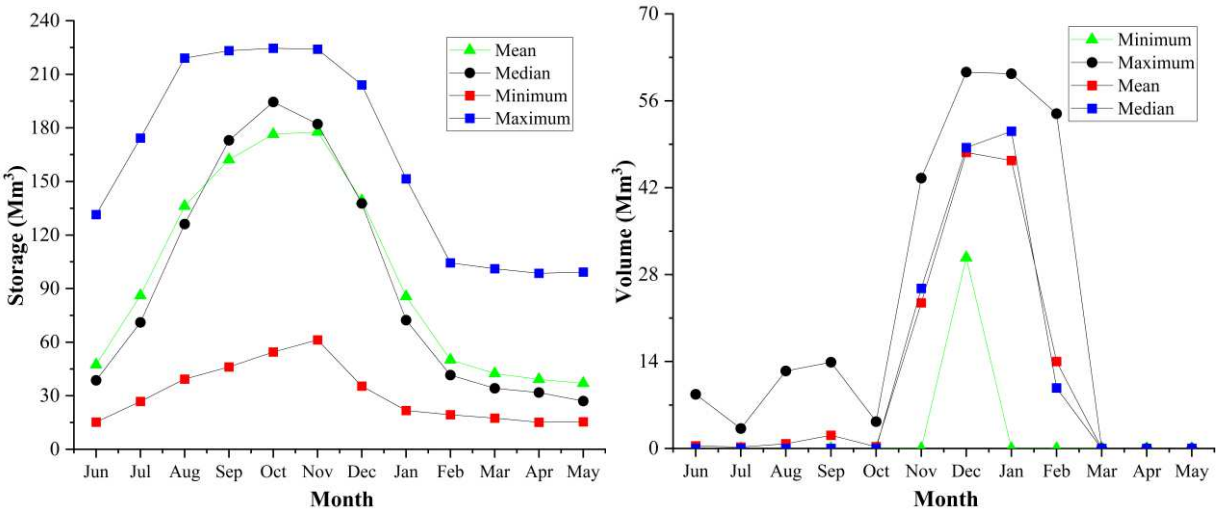


Fig. 3 Annual variation of storage (left) and canal release pattern (right)

2.7 Comparison of spills and deficits of existing and optimized operation

Evaluating the performance of optimized rule curves under both dry and wet conditions is essential to ensure robust and reliable reservoir operation. To achieve this, key performance indicators including spill volumes, irrigation flow deficits, and environmental flow deficits are systematically compared for representative dry and wet years. This comparative assessment enables an objective evaluation of operational effectiveness under varying hydrological conditions. In the present analysis, the period from June 2018 to May 2019 is selected to represent a wet year, characterized by higher inflows, whereas the period from June 2003 to May 2004 is considered a dry year, reflecting reduced water availability. This approach ensures a comprehensive assessment of operational performance across varying inflow regimes.

3. Results

3.1 Convergence of the optimization

The optimization to minimize environmental flow deficit and irrigation flow deficit was carried out using the AMALGM algorithm with variational iterations. Pareto optimal (PO) solution set for the iterations is presented in Fig. 4.

At 10,000 iterations, the PO solutions are few and highly clustered, with many solutions repeating the same objective combinations. The irrigation flow deficit lies within a relatively narrow range of 577.08 Mm^3 to 639.71 Mm^3, and the environmental flow deficit varies only between 0 Mm^3 and 10.31 Mm^3. This limited spread suggests that the optimization converged early to a small region of the objective space, capturing only a restricted set of trade-offs. In comparison, after 10,000,000 iterations, the PO solutions are well-distributed, forming a broader, smoother Pareto front. The irrigation flow deficit ranges from 513.52 Mm^3 to 618.36 Mm^3, while the environmental flow deficit ranges from 0 Mm^3 to 44.78 Mm^3. This fourfold expansion in the environmental flow deficit compared to the 10,000 iterations indicates enhanced exploration of the objective space.

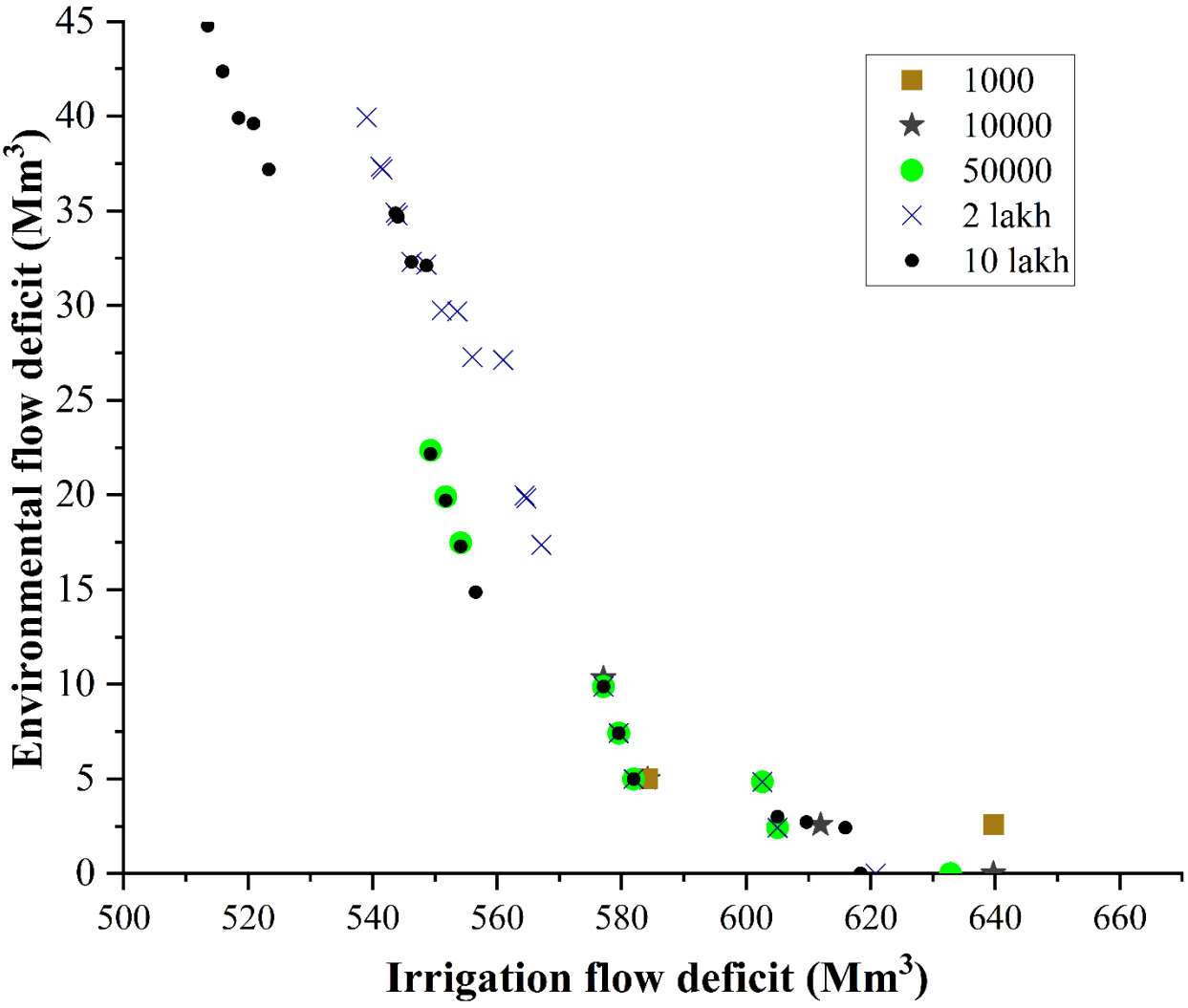


Fig. 4: Pareto optimal solution set for different iterations

The quality of PO solutions with increasing optimization iterations was assessed using the hypervolume indicator (Fig. 5). The hypervolume increases systematically from 0.504 at 1,000 iterations to 0.560 at 10,000 iterations. A more pronounced improvement is observed between 10,000 and 200,000 iterations, where hypervolume increases from 0.560 to 0.667, indicating enhanced coverage and diversity of the Pareto front. Beyond 200,000 iterations, the rate of hypervolume improvement decreases markedly. The hypervolume reaches 0.7196 at both 500,000 and 10,00,000 iterations, with only a marginal increase between the runs. This plateau suggests that the Pareto front has largely converged, and that further iterations primarily refine existing

solutions rather than expand coverage of the objective space. The hypervolume analysis confirms that increasing the number of iterations improves both the convergence and the spread of the PO solution set, with most gains occurring at intermediate iteration counts. Iterations beyond 5,00,000 yield limited additional benefit relative to computational cost, indicating an effective balance between solution quality and optimization efficiency. Finally, from Fig. 4 and 5, it can be concluded that the PO set for 10,00,000 iterations is the convergent solution for the optimization.

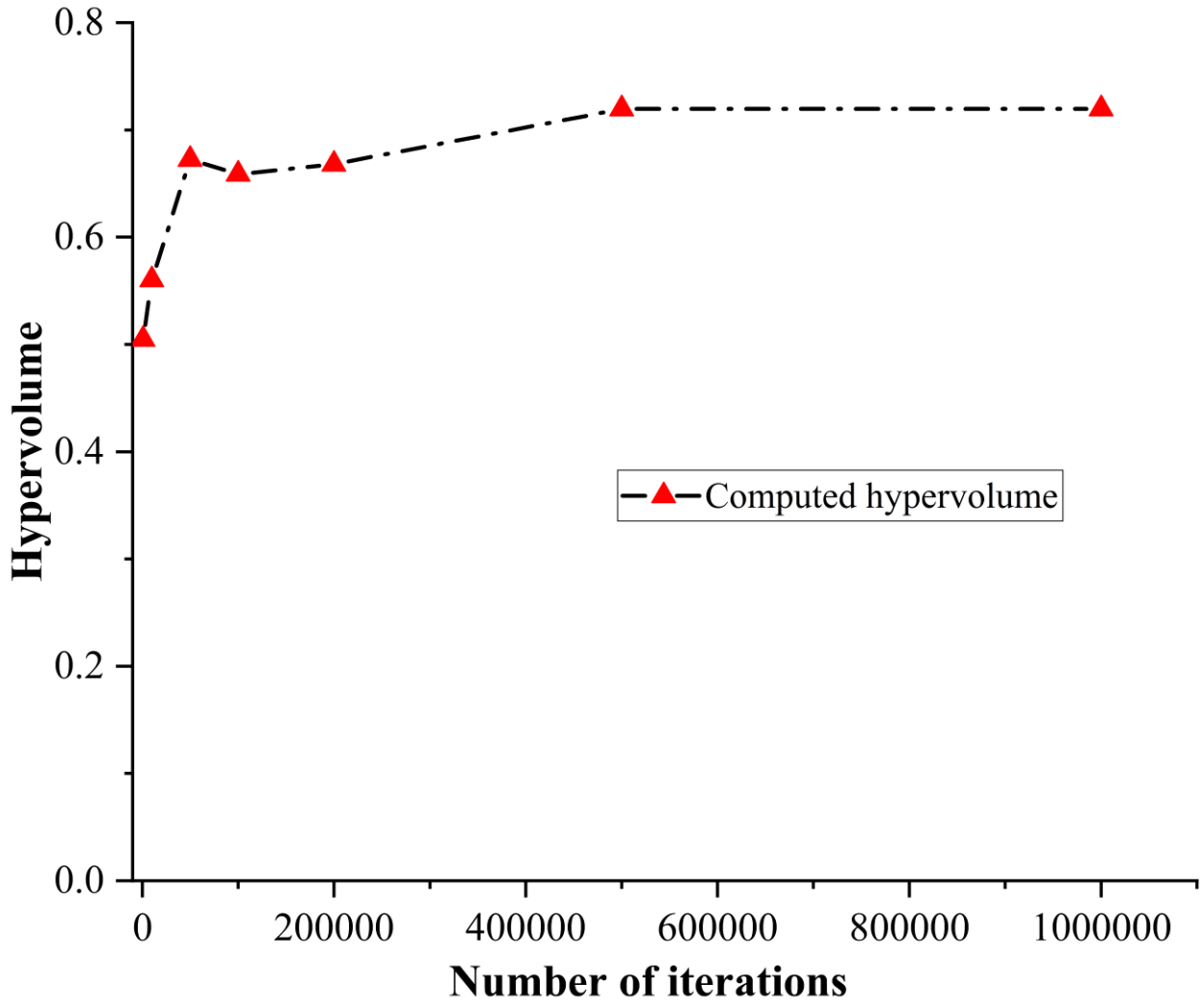


Fig. 5: Variation of hypervolume for different iterations

3.2 Selection of trade-off solutions

Fig. 6 shows the normalized Pareto front and the optimal solutions selected by different methods. The objective function 1 (f1) refers to the irrigation deficit, and the objective function 2 (f2) refers to the environmental flow deficit. The optimal solutions computed by the weighted sum, the knee point, and the ideal point methods coincide, whereas the optimal solution computed by the Achievement Scalarization Function method differs.

The Pareto optimal solution (556.567 Mm^3, 14.860 Mm^3) was consistently selected by the weighted sum, knee point, and ideal point methods, indicating a stable compromise solution located near the central region of the Pareto front. These methods inherently favor balanced trade-offs by either aggregating objectives or minimizing distance to an ideal reference, which explains their convergence toward the same solution. In contrast, the achievement scalarizing function (ASF) method identified a different Pareto optimal solution (554.148 Mm^3, 17.281 Mm^3). This solution provides a marginal improvement in the second objective at the expense of the first objective, reflecting the ASF method's sensitivity to aspiration levels and scaling preferences. Although both the weighted sum and ASF methods assigned equal weights (0.5) to each objective, they produced different Pareto optimal solutions, reflecting the distinct formulations and sensitivities of the methods in exploring the objective space. This divergence highlights how decision-making strategies influence solution selection and underscores the importance of using multiple criteria to fully characterize the trade-off structure of the Pareto front.

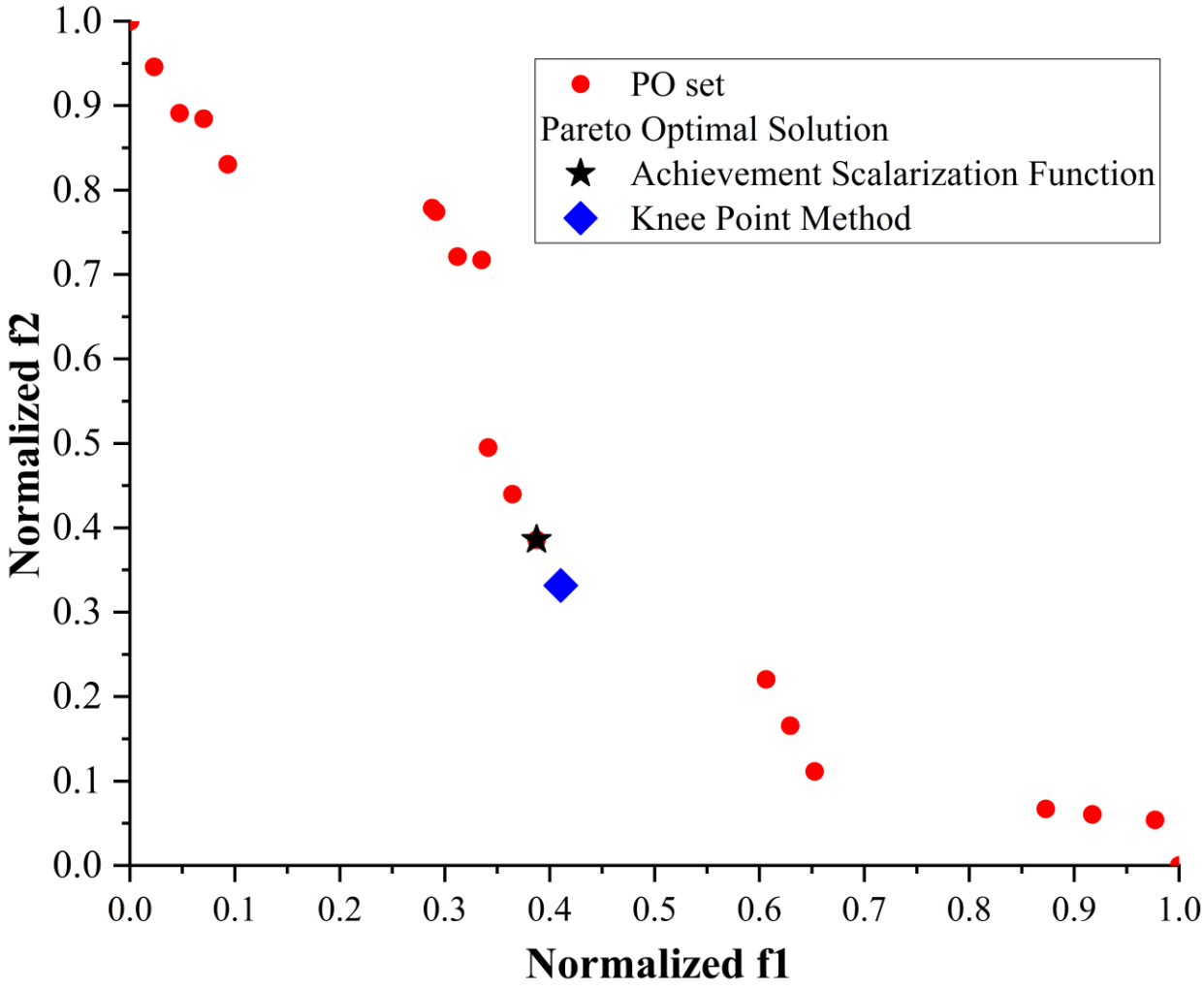


Fig. 6: Selection of trade-off solutions using various methods [The objective function 1 (f1) refers to the irrigation deficit, and the objective function 2 (f2) refers to the environmental flow deficit]

*3.3 **Comparison of trade-off solutions***

The implications of selecting different trade-off solutions are compared. To compare, two additional solutions – one with minimizing f1 alone and another with minimizing f2 alone are computed. It is compared with the tradeoff solution using the Knee Point Method (KPM) and the Achievement Scalarization Function (ASF) method and the results are presented in Fig. 7. The f1 and f2 solutions presented in the figure are similar in nature except for the marked difference in the Upper Rule Curve (URC) in the month of January. The f1 solution resulted in a smaller distance

between the LRC and URC in January. This is due to the minimization of the irrigation deficit (f1) in January, which necessitates a higher release and ultimately brings the URC closer to the Lower Rule Curve (LRC).

The trade-off solutions for KPM and ASF differ in URC during December and January. The URC of KPM is higher than that of ASF in December and January to maintain sufficient storage, allowing irrigation deficits in these months to meet the environmental flow demand in March, April, and May. Thus, the KPM solution tends to be more accommodating of environmental flow needs than the ASF solution. This result is consistent with Fig. 6, which shows that the KPM solution provides a marginal improvement in the second objective compared to the ASF solution.

The comparison of the f1 and f2 solutions with the trade-off solutions of KPM and ASF shows similarities in the URC for August, September, October, and November. This is due to the availability of water during the monsoon months. However, there are differences in the LRC. There is a difference in the URC in June, when the f1 and f2 solutions result in higher release, leading to lower URC than with the KPM and ASF solutions. Overall, trade-off solutions are more suitable for practical decision-making than single-objective optimization solutions, as they provide a balanced representation of competing system objectives.

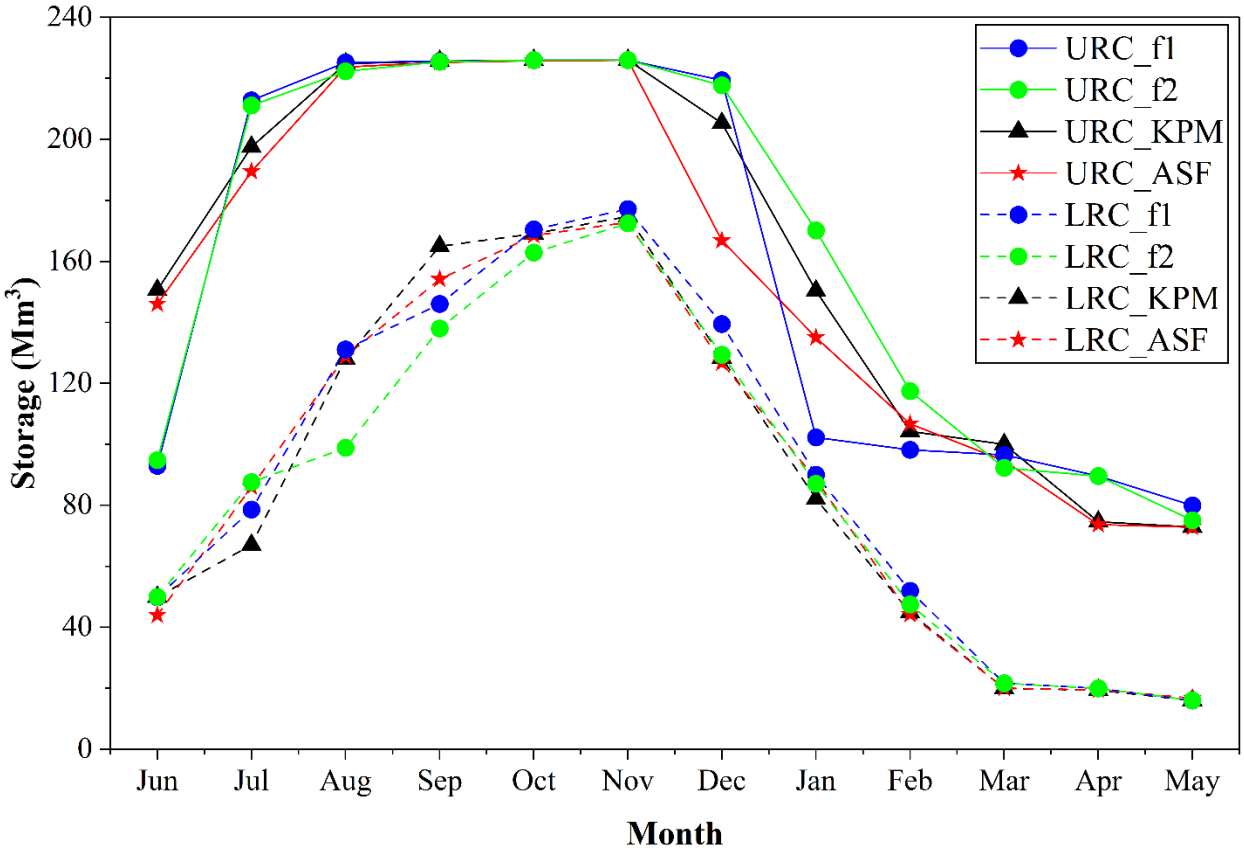


Fig. 7: Comparison of trade-off solutions

3.4 Computation of performance metrics

Table 1 presents the performance indicator values calculated for the historical operation scenario (H1) and the long-term operation scenario (L1). For scenario H1, the time-based reliability values are 0.78 (ASF, KPM) and 0.85 (ASF) -0.90 (KPM) for irrigation and E-flow purposes, respectively, with the optimal rule curves. This implies that the probability of the system remaining in the successful state (without deficit) is 78% for the irrigation operation and 85-90% for the E-flow requirement. In other words, the irrigation and E-flow demands are met for 78% and 85-90% of the operational time horizon, respectively, when the optimal rule curve levels are followed. In the existing operational plan, these values are lower: irrigation reliability is 0.75, and E-flow reliability is 0.50.

Table. 1: Performance indicators – historic and long-term operation

Purpose	Performance indicator	Historic operation (H1 scenario)			Long-term operation (L1 scenario)		
		KPM	**ASF**	**Existing operation**	**KPM**	**ASF**	**Existing operation**
Irrigation	α^I Time Reliability	0.78	0.78	0.75	0.79	0.81	0.75
	β^I Volume Reliability	0.83	0.83	0.83	0.86	0.86	0.85
	γ^I Resilience	0.86	0.86	0.84	0.83	0.83	0.81
	V^I Vulnerability	5.89	5.62	5.71	4.72	4.75	4.97
e-flow	α^E Time Reliability	0.90	0.85	0.50	0.89	0.89	0.53
	β^E Volume Reliability	0.91	0.86	0.54	0.92	0.91	0.58
	γ^E Resilience	0.67	0.55	0.43	0.61	0.60	0.48
	V^E Vulnerability	0.16	0.65	0.78	0.13	0.15	0.71

The volume-based reliabilities for irrigation and E-flow requirements are obtained as 0.83 and 0.86(ASF)-0.91(KPM), respectively, which means that 83% of the total irrigation demands (in terms of volume) and 86-91% of the total E-flow demands are satisfied when the reservoir is operated at the optimal rule curve levels. Although the volume-based irrigation reliability did not improve from its existing value of 0.83, a considerable improvement in the e-flow reliability could be achieved with the optimal operating policy.

The resilience values of 0.86 and 0.55 (ASF)- 0.67 (KPM), respectively, for irrigation and E-flow purposes during optimal rule curve operation indicate that the system can quickly recover from a deficit period to a non-deficit period. The rate at which the reservoir recovers from an irrigation

deficit is faster than that of recovery from an E-flow deficit. According to the existing rule curves, the resilience values were 0.84 and 0.43 for irrigation and e-flow regulation, respectively.

The vulnerability values are calculated as the mean monthly deficit over the operational period. The average deficit is lower for optimized rule curves in both irrigation and E-flow applications. The mean irrigation deficit is reduced from 5.71 Mm^3 to 5.62 Mm^3 when optimized rule curves derived from ASF are followed. The corresponding decrease in e-flow vulnerability is from 0.78 Mm^3 to 0.65 Mm^3. However, the mean irrigation deficit increased to 5.89 Mm^3 with the KPM method, accompanied by a greater reduction in mean e-flow deficits from 0.78 Mm^3 to 0.16 Mm^3.

When the performance of optimized rule curves in long-term operation was analyzed, it was found that time-based irrigation reliability improved from 75% to 79% (KPM)- 81% (ASF) with optimized rule curves, compared to existing rule curve operation, while time-based E-flow reliability increased from 53% to 89%. When the existing rule curve is replaced by the optimal rule curve, the volume-based irrigation reliability increases slightly from 85% to 86%, while E-flow reliability increases considerably from 58% to 91-92%. The long-term irrigation resilience improved slightly from 0.81 to 0.83, while E-flow resilience improved from 0.48 to 0.60 under optimized rule-curve operation. Average irrigation deficits reduced from 4.97 Mm^3 to 4.72 (KPM)-4.75(ASF) Mm^3, and average e-flow deficits from 0.73 Mm^3 to 0.13 (KPM)-0.15(ASF) Mm^3.

3.5 Performance assessment for the historical time period

Fig. 8 illustrates the total reservoir spill volumes during the historical period under both existing and optimized operating policies. A comparative assessment of these results indicates that the total spill associated with the existing operation policy is considerably higher than that observed under the optimized operation policies. Over the 20-year simulation period, the total spill is reduced to

699.27 Mm³ when applying the optimal rule curves derived using the ASF method and to 721.59 Mm³ when using the KPM method, compared with 755.82 Mm³ under the existing rule curves. The maximum annual reduction in spill under both the KPM and ASF methods is 20.08 Mm³, which is about 8.9% of the reservoir capacity, while the average annual reductions are 2.28 Mm³ and 3.37 Mm³, respectively. The decrease in spill in the optimized solution, during the wet years reflects efficient use of available storage capacity and better alignment in balancing subsequent irrigation and environmental deficits. Thus, the water retained within the reservoir under the optimized policies remains available for controlled releases during periods of low inflow. This operational adjustment increases environmental flow (E-flow) supply during dry months while ensuring that reservoir performance remains consistent with established operational and hydrological constraints.

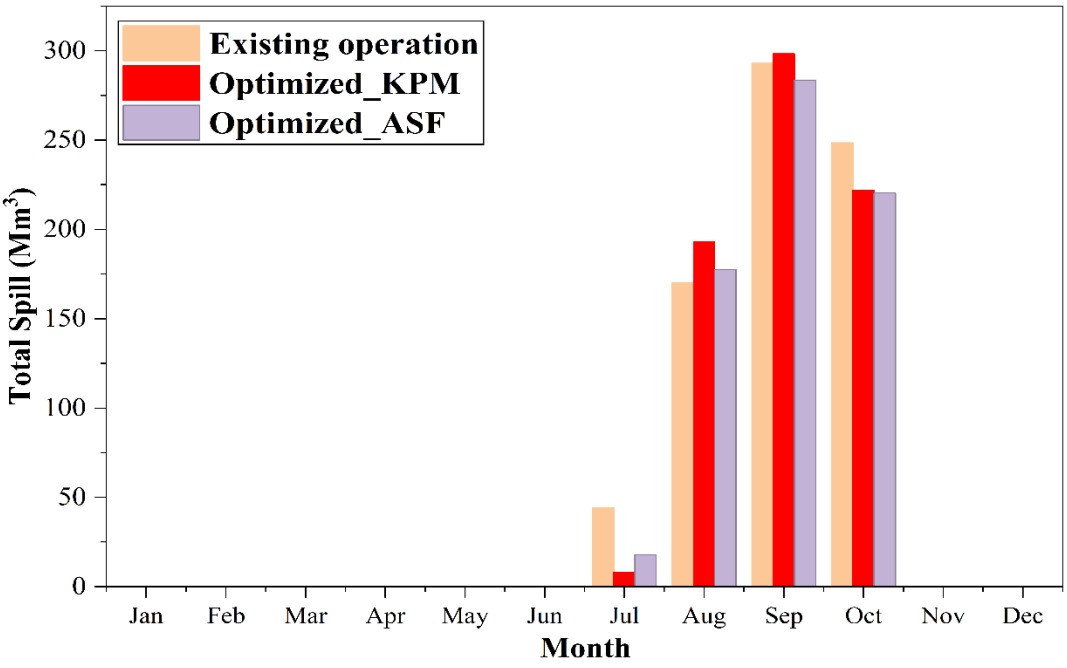


Fig. 8: Comparison of total monthly spills for existing and optimized operation over the 20-year simulation period

3.6 Performance assessment for wet years and dry years

Fig. 9a illustrates the irrigation and environmental flow deficits observed during a representative dry year under both existing and optimized reservoir operating policies. The results show that irrigation deficits remain unchanged for the two operational strategies, indicating that implementing optimized rule curves does not adversely affect the irrigation water supply. For the dry year considered, the total irrigation deficit amounts to 142.85 Mm^3 under both existing and optimized operations. In contrast, notable differences are observed in environmental flow performance. The existing operation results in a total environmental flow deficit of 4.88 Mm^3, whereas no environmental flow deficit occurs when the optimized rule curves are applied. This demonstrates the effectiveness of the optimized operation in meeting environmental flow requirements during dry conditions, even while meeting irrigation requirements. Thus, the proposed model effectively addresses environmental flow requirements without compromising irrigation releases, which is the primary goal of the developed framework.

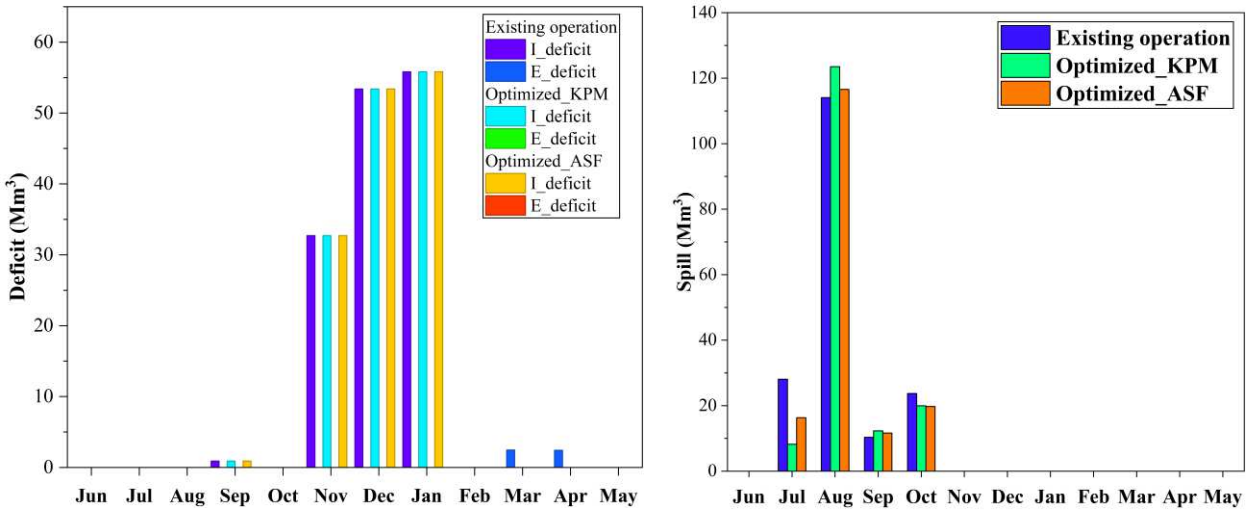


Fig. 9: Variation in a) total deficit in dry year (left) and b) total spill in wet year (right)

Fig. 9b presents a comparison of reservoir spill volumes under existing and optimized rule curves for a representative wet year. Under the existing operation plan, the total spill during the period amounts to 176.16 Mm^3. When the optimized rule curves are implemented, a reduction in spill volume is observed. Specifically, the spill volume decreases to 164.25 Mm^3 when using the ASF-derived rule curves and to 164 Mm^3 when applying the KPM-derived rule curves. This reduction indicates that the optimized operating policies enable more effective regulation of reservoir releases during high inflow conditions, which are typical of wet years. The lower spill volumes achieved under both optimization methods demonstrate improved utilization of reservoir storage capacity compared to the existing rule curves.

Overall, the results indicate that the proposed optimal rule curves consistently reduce reservoir spill volumes when compared with the existing operation policy. This improvement is observed across representative dry years (Fig. 9a), wet years (Fig. 9b), and the complete historical simulation period (Fig. 8), demonstrating the effectiveness of the optimized rule curves under a wide range of hydrological conditions.

4. Discussion

The present study emphasizes the applicability of AMALGAM in deriving optimal trade-offs for irrigation and ecological operations of a conservation reservoir by modifying its rule curve parameters. The use of AMALGAM for rule curve derivation significantly reduces the problem's dimensionality and, simultaneously, provides Pareto-optimal solutions within a single optimization run, resulting in reduced computational time. Though the multi- algorithm search capability of AMALGAM has been utilized in the design of water distribution systems (Raad et al., 2010), calibration of hydrologic models (Koppa et al., 2019; Besalatpour et al., 2023),

groundwater remediation (Ouyang et al., 2017), the application of this algorithm to reservoir operation optimization is limited to flood control optimization (Duraisekharan et al., 2025).

The application of the proposed methodology to the case study of the Malampuzha reservoir demonstrates an efficient method for allocating minimum environmental flows from an irrigation reservoir that lacks an exclusive rule curve for environmental flows. Under the existing reservoir operation plan, e-flows were provided only when sufficient storage was available, resulting in high e-flow deficits during dry years. This is rectified by the optimal rule curves, as evidenced by higher reliability values for e-flows compared to the existing operation plan. This indicates that the optimized operation plan ensures minimal environmental flows even during the dry months by maintaining higher values on the lower rule curves during the dry period of the year. The upper rule curve in the monsoon period is also modified from the existing rule curves, resulting in reduced spill and increased water availability to meet E-flow requirements. Optimizing the rule curve levels of the Malampuzha reservoir to provide minimum environmental flows during dry periods is advantageous for reservoir operators and managers, particularly in the context of increasing drought trends in the region (George, 2020; Rose and Chithra, 2022). By using the 75^{th} percentile values of irrigation and environmental flow demand to derive the rule curves, the model ensures manageable e-flow standards, neither too low for a dry year nor too high for a wet year. Additionally, the post-processing of the Pareto front using various classical selection methods is discussed, which can facilitate the selection of a practical optimal solution and thereby avoid the complexities associated with multi-criteria decision-making models. Two alternative solutions are provided with the KPM and ASF methods, among which the KPM-derived rule curves provide more water for environmental flow requirements at the cost of irrigation deficits in January and December, while the ASF–derived rule curves allow for environmental flow deficits without

compromising irrigation demand much. Thus, the proposed optimal rule curves provide reservoir operators with the opportunity to choose the most suitable operational plan based on prevailing field conditions.

The optimization model proposed uses the 75^{th} percentile of the historical E-flow releases as the ecological demand, as adequate data for calculating downstream ecological demands is not available. The model is advantageous in the case of rivers where adequate data on downstream ecological flow parameters are not available or a separate rule curve does not exist for the reservoir to meet ecological demands, as it can provide a quick reference for setting the target rule curve levels for a minimum E-flow regime without compromising much on the irrigation demands. Including indicators of hydrologic alteration in the calculation of ecological demands can improve the model's accuracy.

5. Conclusions

The rule curve levels of a conservation reservoir are optimized to minimize irrigation and environmental flow deficits simultaneously using AMALGAM, a genetic algorithm-based search technique. Four methods were used to select optimal solutions from the Pareto front. The results show that the optimized rule curve levels can reduce the irrigation and environmental flow deficits by 63% and 79%, respectively, over the historic 20-year period studied. A reduction in spill volume could also be achieved by following the optimized rule curve levels. The performance of the proposed rule curves is robust across the entire operational horizon, as evidenced by results from a wet year and a dry year. For a dry year, the environmental flow demands could be fully satisfied with the optimal rule curves, while the existing rule curve could supply only 3% of the e-flow

demand. Similarly, for a wet year, the total spill volume could be reduced by about 7% with the optimal rule curves. Reduction in spill volume and reduction in environmental flow deficits were fulfilled without compromising on the irrigation objective. The proposed rule curve levels perform well in the long-term operation as well. This is evident from the reliability, resilience, and vulnerability values obtained during long-term operation.

Optimized rule curve levels can help reservoir operators manage available storage to reduce irrigation and environmental flow deficits simultaneously. The developed methodology can be applied to conservation reservoirs to modify the existing rule curves to incorporate the environmental flow requirements.

Declarations

Ethical Approval Not applicable.

Consent to Participate Not applicable.

Consent to Publish

The authors declare their consent of the publication of this manuscript by "Water Resources Management" journal.

Author Contributions

Balaji Narasimhan, Sudheer K. P., Sarmistha Singh, Athira P., and Subhasis Mitra contributed to the conceptualization and methodology development. Balaji Narasimhan, Sarmistha Singh, Athira P., and Subhasis Mitra supervised the study. Formal analysis and investigation were conducted by Sukanya J. Nair and Elanchezhiyan Duraisekaran. Sukanya J. Nair prepared the original draft of the manuscript. The manuscript was reviewed and edited by Sukanya J. Nair, Elanchezhiyan

Duraisekaran, Balaji Narasimhan, and Sarmistha Singh. All authors contributed to the discussion of the results and approved the final version of the manuscript.

Acknowledgement

The authors acknowledge the contributions of the research staff Ms. Aswathy M., Mr.Swarnadeep Mukherjee and Ms. Shree Madhumathy.

Funding

The authors thank the Irrigation Design and Research Board, Government of Kerala for providing the necessary data and financial support.

Competing Interests

The authors declare no conflict of interest.

Availability of Data and Materials

Datasets are available upon request.

References

A. Thomas, J., & B Fiering, M. (1962). Mathematical synthesis of streamflow sequences for the analysis of river basins by simulation. In *Design of water-resource systems: new techniques for relating economic objectives, engineering analysis, and governmental planning* (pp. 459-493). Harvard University Press.

Besalatpour, A. A., Pourreza-Bilondi, M., & Aghakhani Afshar, A. (2023). Parallelization of AMALGAM algorithm for a multi-objective optimization of a hydrological model. *Applied Water Science*, *13*(12), 241.

Beume, N., Naujoks, B., & Emmerich, M. (2007). SMS-EMOA: Multiobjective selection based on dominated hypervolume. *European journal of operational research*, *181*(3), 1653-1669.

Chen, M., Dong, Z., Jia, W., Ni, X., & Yao, H. (2019). Multi-objective joint optimal operation of reservoir system and analysis of objectives competition mechanism: a case study in the upper reach of the Yangtze River. *Water*, *11*(12), 2542.

Crespo, D., Albiac, J., Kahil, T., Esteban, E., & Baccour, S. (2019). Tradeoffs between water uses and environmental flows: a hydroeconomic analysis in the Ebro Basin. *Water Resources Management*, *33*(7), 2301-2317.

Dittmann, R., Froehlich, F., Pohl, R., & Ostrowski, M. (2009). Optimum multi-objective reservoir operation with emphasis on flood control and ecology. *Natural Hazards and Earth System Sciences*, *9*(6), 1973-1980.

Dunn, S. M., Stalham, M., Chalmers, N., & Crabtree, B. (2003). Adjusting irrigation abstraction to minimise the impact on stream flow in the East of Scotland. *Journal of environmental management*, *68*(1), 95-107.

Duraisekaran, E., Kumar, K., Bindhu, V. M., & Narasimhan, B. (2024). A Simulation-Optimization Framework for Effective Flood Management in a Conservation Reservoir.

Duraisekaran, E., Kumar, K., Bindhu, V. M., & Narasimhan, B. A Simulation-Optimization Framework for Effective Flood Management in a Conservation Reservoir.

Fallah-Mehdipour, E., Bozorg-Haddad, O., & Loáiciga, H. A. (2018). Calculation of multi-objective optimal tradeoffs between environmental flows and hydropower generation. *Environmental Earth Sciences*, *77*, 1-10.

George, J. (2020). Long-term changes in climatic variables over the Bharathapuzha river basin, Kerala, India. *Theoretical & Applied Climatology*, *142*.

Jain, S. K., & Bhunya, P. K. (2008). Reliability, resilience and vulnerability of a multipurpose storage reservoir. *Hydrological sciences journal*, *53*(2), 434-447.

Jiang, Z., Liu, P., Ji, C., Zhang, H., & Chen, Y. (2019). Ecological flow considered multi-objective storage energy operation chart optimization of large-scale mixed reservoirs. *Journal of Hydrology*, *577*, 123949.

Jincy Rose, M. A., & Chithra, N. R. (2022). Establishing a statistical relation between meteorological and hydrological drought indices. *Water Supply*, *22*(4), 4262-4277.

Jo, Y. J., Song, J. H., Her, Y., Provolo, G., Beom, J., Jeung, M. & Yoon, K. S. (2021). Assessing the potential of agricultural reservoirs as the source of environmental flow. *Water*, *13*(4), 508.

Jose, R., & Srinivasan, K K, S. (2025a). Multi-Objective Modeling Framework for Environmental Flow Optimization in a River-Reservoir System Using Histogram Comparison Approach for Estimation of Hydrologic Alteration. : R. Jose, S. K. *Water Resources Management*, 39(1), 439-458.

Jose, R., & Srinivasan, K. (2025b). Two-stage Adaptive Modelling Framework for Long-term Monthly Operation of a Multi-purpose Reservoir for Regulating Environmental Flows. *Water Resources Management*, 1-19.

KhazaipPoul, A., Moridi, A., & Yazdi, J. (2019). Multi-objective optimization for interactive reservoir-irrigation planning considering environmental issues by using parallel processes technique. *Water Resources Management*, *33*, 5137-5151.

Kjeldsen, T. R., & Rosbjerg, D. (2004). Choice of reliability, resilience and vulnerability estimators for risk assessments of water resources systems. *Hydrological sciences journal*, *49*(5).

Koppa, A., Gebremichael, M., & Yeh, W. W. (2019). Multivariate calibration of large- scale hydrologic models: The necessity and value of a Pareto optimal approach. *Advances in Water Resources*, *130*, 129-146.

Kundzewicz, Z. W., & Kindler, J. (1995). Multiple criteria for evaluation of reliability aspects of water resource systems. *IAHS Publications-Series of Proceedings and Reports-Intern Assoc Hydrological Sciences*, *231*, 217-224.

López, A., Zapotecas, S., Coello, C. A., Abraham, A., Jain, L., & Goldberg, R. (2009). An introduction to multiobjective optimization techniques. *Evolutionary multiobjective optimization: Theoretical advances and applications*, 7-32.

Marler, R. T., & Arora, J. S. (2010). The weighted sum method for multi-objective optimization: new insights. *Structural and multidisciplinary optimization*, *41*, 853-862.

Ngoc, T. A., Hiramatsu, K., & Harada, M. (2014). Optimizing the rule curves of multi-use reservoir operation using a genetic algorithm with a penalty strategy. *Paddy and Water environment*, *12*, 125-137.

Null, S. E., Olivares, M. A., Cordera, F., & Lund, J. R. (2021). Pareto optimality and compromise for environmental water management. *Water Resources Research*, *57*(10)., e2020WR028296.

Ouyang, Q., Lu, W., Hou, Z., Zhang, Y., Li, S., & Luo, J. (2017). Chance-constrained multi-objective optimization of groundwater remediation design at DNAPLs-contaminated sites using a multi-algorithm genetically adaptive method. *Journal of contaminant hydrology*, *200*, 15-23.

Pang, A., Li, C., Sun, T., Yang, W., & Yang, Z. (2018). Trade-off analysis to determine environmental flows in a highly regulated watershed. *Scientific Reports*, *8*(1), 14130.

Qi, P., Tang, X., Xu, Y. J., Cui, Z., Sun, J., Zhang, G. & Jiang, M. (2023). Optimizing environmental flow based on a new optimization model in balancing objectives among river ecology, water supply and power generation in a high-latitude river. *Journal of Environmental Management*, *342*, 118261.

Raad, D. N., Sinske, A. N., & Van Vuuren, J. H. (2010). Comparison of four reliability surrogate measures for water distribution systems design. *Water Resources Research*, *46*(5).

Sunil, A., Singh, R., & Molakala, M. (2024). Adaptive (re) operations facilitate environmental flow maintenance downstream of multi-purpose reservoirs. *Journal of Hydrology*, *644*, 132123.

Taghian, M., Rosbjerg, D., Haghighi, A., & Madsen, H. (2014). Optimization of conventional rule curves coupled with hedging rules for reservoir operation. *Journal of Water Resources Planning and Management*, *140*(5), 693-698.

Vrugt, J. A., & Robinson, B. A. (2007). Improved evolutionary optimization from genetically adaptive multimethod search. *Proceedings of the National Academy of Sciences*, *104*(3), 708-711.

Wang, Y., Wang, D., & Wu, J. (2015). Assessing the impact of Danjiangkou reservoir on ecohydrological conditions in Hanjiang river, China. *Ecological Engineering*, *81*, 41-52.

Wineland, S. M., Başağaoğlu, H., Fleming, J., Friedman, J., Garza-Diaz, L., Kellogg, W. & Wootten, A. M. (2022). The environmental flows implementation challenge: Insights and recommendations across water-limited systems. *Wiley Interdisciplinary Reviews: Water*, *9*(1), e1565.

Yazdian, H., Zahraie, B., & Jaafarzadeh, N. (2024). Multi—Objective Reservoir Operation Optimization by Considering Ecosystem Sustainability and Ecological Targets. *Water Resources Management*, *38*(3), 881-892.

Yin, X. A., Yang, Z. F., & Petts, G. E. (2012). Optimizing environmental flows below dams. *River research and applications*, *28*(6), 703-716.

Zhang, X., Tian, Y., & Jin, Y. (2014). A knee point-driven evolutionary algorithm for many-objective optimization. *IEEE transactions on evolutionary computation*, *19*(6), 761-776.

Zhou, Y., & Guo, S. (2013). Incorporating ecological requirement into multipurpose reservoir operating rule curves for adaptation to climate change. *Journal of Hydrology*, *498*, 153-164.